

Original Article

Enhancing Fingerprint Image Resolution Using Auto-Encoder and Interpolation Techniques

P.P. Lisha¹, V.K. Jayasree²

^{1,2}Department of Electronics and Communication Engineering, Model Engineering College Research Centre, Cochin University of Science and Technology, Kerala, India.

¹Corresponding Author : lishap.p@outlook.com

Received: 12 February 2024

Revised: 12 March 2024

Accepted: 10 April 2024

Published: 30 April 2024

Abstract - Super-Resolution (SR) techniques play a vital role in enhancing the resolution of low-quality images, including fingerprint images, which are crucial for various applications such as biometric authentication and forensic analysis. However, achieving high-quality super-resolution of fingerprint images poses several challenges, including preserving fine details and minimizing artifacts. Existing methods often struggle to effectively enhance fingerprint images without sacrificing important features or introducing unwanted distortions. This study presents a novel approach for enhancing the resolution of low-resolution fingerprint images to high-resolution ones using an auto-encoder in combination with spline and bi-cubic interpolation methods. For effective analysis in a variety of applications, including satellite photography, surveillance, and medical imaging, high-quality images are imperative. However, the transmission, storage, and processing of high-resolution images require substantial bandwidth, storage, and computational resources. Therefore, there is a need for computationally efficient and size-optimized resolution enhancement algorithms. The proposed method enhances fingerprint images from a size of 129×97 to 258×194 . Utilizing spline and bi-cubic interpolation techniques ensures smoother curves and reduced artifacts during image up-sampling, preserving fidelity and detail. The model is trained on the FVC 2004 dataset and tested on both FVC 2004 and FVC 2002 datasets. Performance evaluation metrics such as SSIM, PSNR, and MSE yielded values of 35.14, 0.968, and 0.007, respectively. Furthermore, the identification accuracy of the proposed model, measured using the SIFT algorithm, achieved 100% on these datasets. The outcomes of the experiment show the effectiveness and superiority of the proposed approach in enhancing fingerprint image resolution, paving the way for improved accuracy and reliability in fingerprint recognition systems.

Keywords - Fingerprint, Super Resolution, Auto encoder, Bi-cubic, Spline interpolation, Minutiae.

1. Introduction

Fingerprints serve as a widely recognized and universally recognized biometric identifier for personal verification, finding applications from smartphone unlocking to border control [1]. This unique trait has garnered significant interest from researchers and industry alike, owing to its familiarity and widespread adoption in various authentication scenarios.

In digital image processing and analysis, fingerprints have diverse applications. High-resolution images are crucial in forensic analysis, facilitating more accurate fingerprint matching and identification and offering enhanced insights for forensic investigations [2].

In the process of automatically identifying fingerprint images, the initial step involves capturing an image of the fingerprint utilizing a sensor like an optical or capacitive scanner [3]. This sensor captures detailed impressions of the fingerprint's ridges and valleys. The distinctive ridge-valley patterns found on fingerprints serve as a basis for personal

identification in a variety of scenarios. Distinctive traits are extracted during enrolment and saved as templates in databases for fingerprint-based identification systems. This template-based approach allows for efficient storage and comparison while ensuring a high degree of accuracy in fingerprint identification [4]. These traits are then compared with input fingerprint data during authentication.

Subsequently, the captured image undergoes pre-processing to enhance its quality and extract essential features for identification purposes. An important step in this procedure is feature extraction. Many fingerprint traits can be extracted, with minutiae being a prominent choice [5].

Minutiae are anomalies in the ridge-valley pattern that are distinguished by their orientation and location. However, image quality has a major impact on minutiae extraction accuracy. Low-quality fingerprint images are frequently caused by factors such as skin disorders, moisture levels, subject disposition, and scanner pressure.



Consequently, this leads to inaccurate minutiae extraction, which negatively impacts the performance of the authentication system. Particularly on systems with limited resources, high-resolution images can put a load on memory and storage. Super-resolution algorithms are, therefore, essential. These techniques are vital for extracting fine details and minutiae from low-resolution fingerprint images. They successfully recover important data that could otherwise be lost by improving the resolution [6]. This feature ensures that even low-quality images can be used efficiently for fingerprint analysis and recognition, which is especially useful in situations when storage or memory limits exist.

Before authentication, fingerprint images are improved in order to overcome these difficulties. Conventional techniques emphasize ridge-valley contrast enhancement and noise reduction [7]. This research suggests an enhancement method based on Super-Resolution (SR) [8] to further enhance the quality of fingerprint images. Super-resolution is an essential approach in reconstructing high-quality images from one or more low-quality counterparts, making it a focal point in image processing research.

On the basis of their methodological approach, number of images used, and domain, SR approaches are categorized. Spatial and Frequency domain algorithms differ in their operational basis [9]. Adjusting parameters and interpreting intermediate results is made easier by the direct manipulation of pixels by spatial domain algorithms. In contrast, complex mathematical transformations and algorithms are used in frequency domain techniques, which result in significant computational expenses. Because of these differences, SR approaches can be understood more deeply. Spatial domain methods are flexible and easy to grasp, but frequency domain methods require a lot of processing power because of their intricate mathematical processes [10].

SR is divided into two categories based on the number of input images: Single Image SR (SISR) and Multiple Images SR (MISR) [11]. SISR entails transforming one low-quality input into a high-quality image [12], while MISR reconstructs a high-quality image using multiple low-quality inputs. SISR methods employ learning algorithms to exploit the inherent connection between Low-Resolution (LR) and High-Resolution (HR) images, extracting missing details to enhance image quality. These techniques leverage patterns within LR images to infer corresponding HR details, effectively reconstructing super-resolved images with improved visual fidelity by understanding the relationship between LR and HR representations, these algorithms.

The focus of the proposed study lies on SISR to enhance fingerprint images, intending to enhance image quality, facilitate reliable fingerprint feature extraction, and minimize authentication errors. The study's ultimate goal is to develop an algorithm that efficiently enhances fingerprint data

resolution while reducing storage requirements, thereby enhancing automatic identification accuracy in fingerprinting processes.

This paper is organized as follows in the following sections: The relevant literature is examined in section 2. The network architecture and experimental findings are outlined in sections 3 and 4, respectively. Lastly, section 5 encapsulates the conclusion.

2. Related Works

The estimation of the mapping between low-resolution and high-resolution images is greatly aided by SISR. The research community has shown a great deal of interest in image SR recently. Researchers have introduced numerous algorithms based on image super-resolution, resulting in significant advancement since the introduction of deep learning.

Vonderfecht and Liu (2022) [13] investigated fingerprinting in Single-Image Super-Resolution (SISR) networks, finding that networks with high-up scaling or adversarial training exhibit individuality. Using ConvNext for classification, they examined five hyperparameters in 205 SISR models. Their research showed that more recognizable fingerprints were produced via open-ended synthesis tasks. Under some circumstances, model parsing was feasible.

In order to improve periocular verification, Tapia et al. (2022) [14] investigated selfie-based biometrics by utilizing Super-Resolution (SR). They achieved outstanding results by balancing efficiency and filter size in their Efficient Single Image Super-Resolution method. Their approach produced Equal Error Rates (EER) of 8.89% for FaceNet, 12.14% for VGG Face, and 12.81% for ArcFace with fewer parameters. However, even though SR enhanced image quality, issues like uncontrolled environments persisted.

OSRCycleGAN was developed by Lee et al. (2022) [15] for the purpose of ocular super-resolution reconstruction and recognition enhancement. Better recognition rates were obtained by experimenting with the CASIA-iris-Distance, IIT Delhi iris databases, and Lamp v4: 3.02%, 2.13%, and 4.06%, respectively. In comparison to CycleGAN, OSRCycleGAN showed 322% and 161% higher processing speeds on desktop and Jetson TX2, respectively. OSRCycleGAN has shown significant proportionate EER reductions despite modest Equal Error Rate (EER) reductions. One drawback is that there were difficulties in modifying OSRCycleGAN to accommodate various biometric modalities.

Shahbakhsh et al. (2022) [16] proposed a face super-resolution technique using deep learning with the goal of improving face identification accuracy on low-resolution images. They used a Generative Adversarial Network to rebuild high-frequency information and take into account

image edges in order to preserve facial structure. Evaluation against cutting-edge techniques like DFDNet, EIPNet, and GFP-GAN showed improved accuracy in face recognition.

For SISR, Muhammad et al. (2021) [17] presented a multi-path deep CNN with Residual and Inception Network. They employed ResNet, Inception, and deconvolution layers for upscaling in their three-branch model. Results showed a 62% decrease in parameters compared to DRCN and a superior PSNR improvement of 1.88 dB over the baseline bicubic technique on the SET5 dataset at an 8x upscale factor. Nevertheless, computational speed and cost remained limited.

In order to handle low-resolution biometric images, Huang et al. (2021) [18] developed DDA-SRGAN, a GAN-based SR approach with dual-dimension attention. By autonomously identifying regions of interest in LR images, the model improved feature details that are essential for biometric recognition. Experiments conducted on the CASIA-Thousand-v4 and CelebA datasets demonstrated a 0.5% increase in verification rates for iris identification, indicating an improvement above MA-SRGAN performance. The absence of mask attention modules in the model limited its ability to stabilize face recognition, potentially impacting overall performance.

A pore feature-based method for HR fingerprint detection was developed by Anand and Vivek (2020) [19]. They calculated descriptors using PoreNet, a CNN model and used DeepResPore to detect pores. Impressive results were obtained from testing on the PolyU HRF dataset: 2.91% and 0.57% EERs on partial (DBI) and complete (DBI) fingerprints, respectively. The values of FMR1000 and FMR10000 were significantly less than the state-of-the-art. PoreNet demonstrated its potential for high-resolution fingerprint recognition by effectively generating descriptors.

Ngoc Tuyen Le et al. (2020) [20] developed an algorithm for fingerprint image enhancement. Their method utilized Adaptive Higher-Order Singular Value Decomposition on Wavelet Subbands (AHTWF) to improve image quality. Through three stages, they decomposed input images, constructed a tensor, and applied compensation based on a Gaussian template. Experimental results demonstrated significantly enhanced image quality, with clearer ridge structures and removal of background and blur.

Karabulut et al. (2020) [21] employed Cycle-GAN for unpaired image-to-image translation, converting distorted fingerprints (dry, wet, dotted, damaged, blurred) to undistorted counterparts. Utilizing a database of 11,541 samples, they evaluated enhancement via VGG16-based CNN, achieving a peak of 94% accuracy in detecting undistorted wet fingerprints. Real-world data from VISA centers in South America validated the algorithm's effectiveness. Cycle-GAN's symmetric transfer yielded notable quality improvements, particularly for wetness, although blurred fingerprints showed the least enhancement.

3. Materials and Methods

The proposed methodology, as shown in Figure 1, begins with a series of pre-processing steps aimed at preparing the input data for super-resolution enhancement. Initially, the input image of size 258 x 194 undergoes downsampling using bilinear interpolation, resulting in a half-sized image (129 x 97).

Next, bicubic interpolation is applied to the downscaled image to enlarge it back to its original size, serving as input 1 for the auto encoder. Simultaneously, spline interpolation is applied to another downscaled image, creating input 2. Additionally, the down-sampled image from the first step remains unchanged as input 3.

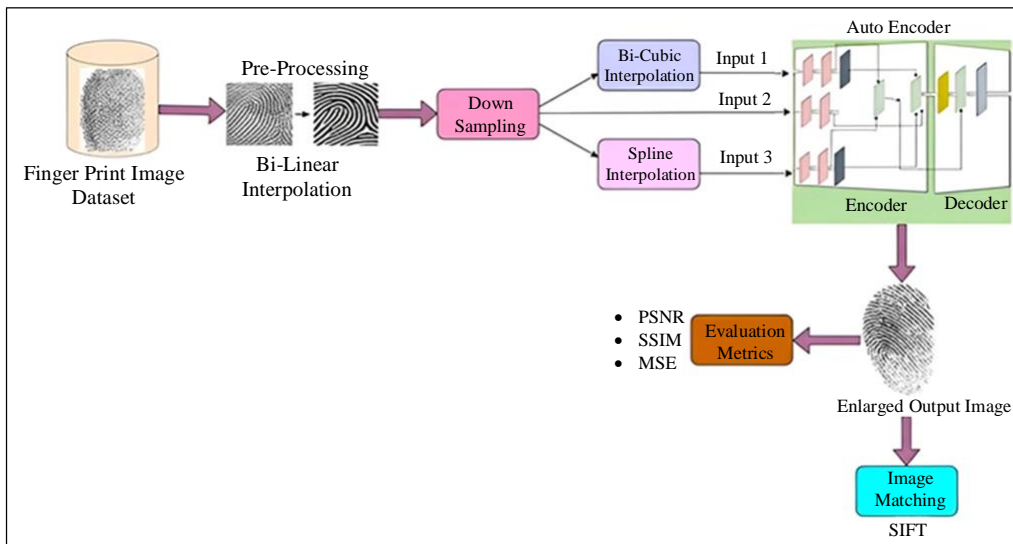


Fig. 1 A block diagram illustrating the proposed approach

Subsequently, the encoder and decoder portions comprise the auto-encoder network. In the encoder section, each input image is subjected to a series of convolutional layers for feature extraction, followed by max-pooling operations to reduce dimensionality.

The extracted features are concatenated to form a latent space. The outputs from these operations are concatenated to capture both high-level and low-level features. In the decoder section, the concatenated features are up-sampled and combined with previous features through concatenation, followed by transposed convolution to generate the final super-resolved output image. Performance evaluation metrics such as MSE, PSNR, as well as SSIM are computed to assess the superiority of the reconstructed image.

Additionally, the fingerprint-matching accuracy between the reconstructed and original images is evaluated using the SIFT algorithm, which measures key feature points and calculates the degree of matching based on the Euclidean distance between similar points. Through this methodology, the autoencoder effectively enhances the resolution of the input images while preserving important details and features, thereby achieving improved image quality.

3.1. Dataset

FVC 2002 [22] and FVC 2004 [23] datasets are used in the proposed study for analysis. Benchmarks for fingerprint recognition research are frequently derived from the Fingerprint Verification Competition (FVC) datasets.

The FVC2004 multi-database collection consists of several datasets that were collected from fingerprints using various sensor technologies. There are four distinct datasets in the FVC2004 fingerprint database, designated DB1, DB2, DB3, and DB4. Table 1 displays the dataset’s description, while Figure 2 displays some of the database’s image samples.

3.2. Data Pre-Processing and Downsampling

In the proposed study, the pre-processing of fingerprint images involves several steps to prepare them for further analysis within the auto encoder network. Initially, the input fingerprint images undergo normalization, where the pixel values are scaled to fall within the range of [0, 255]. Firstly, the pixel values of the fingerprint images are typically extracted, ranging from 0 (black) to 255 (white) in a grayscale format. Then, normalization is applied, which involves linearly mapping the original pixel values to the desired range of [0, 255]. This normalization step ensures consistency and comparability of pixel intensities across all images in the dataset. Following normalization, the images with dimensions 258 x 194 pixels are subjected to downsampling using bilinear interpolation, reducing their size by half with dimensions 129 x 97 pixels. Bilinear interpolation [24] involves considering the surrounding four-pixel values alongside distance weights to compute the new interpolated value for a given pixel point, as shown in Figure 3.

$$f(x + u, y + v) = (1 - u)(1 - v)f(x, y) + u(1 - v)f(x + 1, y) + v(1 - u)f(x, y + 1) + uvf(x + 1, y + 1) \quad (1)$$

Equation 1 is employed to calculate the value at coordinates (x + u, y + v), where x and y stand for the input fingerprint image’s row and column coordinates of the known locations correspondingly. The variables u and v denote the differences in distance between the desired point and the known point’s row and column coordinates correspondingly. This method ensures smooth interpolation of pixel values across the resized image, preserving some of the essential features of the original image while reducing its resolution. This downscaled image serves as the basis for further processing within the proposed methodology, facilitating subsequent operations such as bicubic and spline interpolation, as well as feature extraction through convolutional layers in the auto-encoder network.

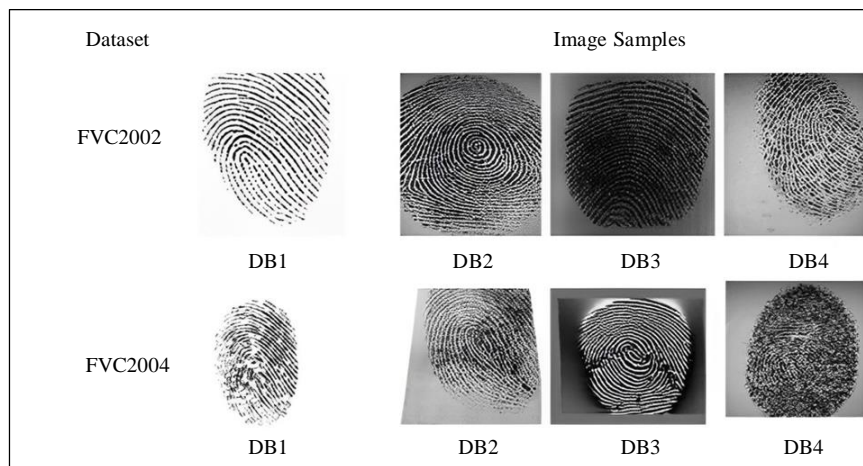


Fig. 2 Sample images of dataset

Table 1. Dataset description

Dataset	Resolution	Size
FVC 2004	500 dpi	328 X 364, 640 X 480, 300 X 480
FVC 2002	500 dpi	300 X 300, 388 X 374, 296 X 560

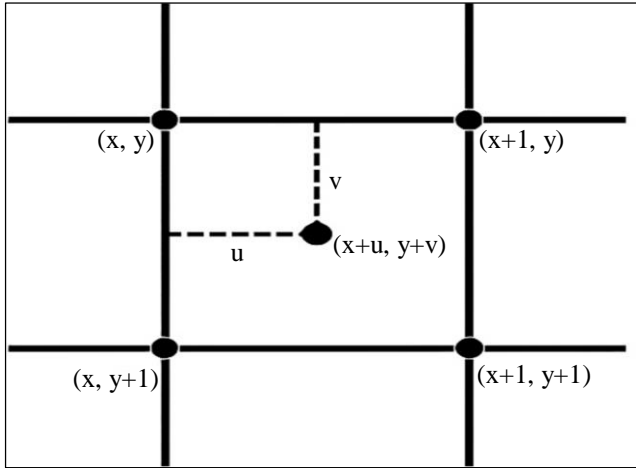


Fig. 3 Diagrammatic representation of the bilinear interpolation technique

3.3. Interpolation Techniques

Following downsampling, bicubic and spline interpolations are performed on separate downscaled images. Bicubic interpolation involves estimating new pixel values by considering the surrounding sixteen pixels in a 4x4 neighborhood and their respective distance weights. This method ensures a smooth and continuous transition between neighbouring pixels, resulting in enhanced image quality. Bicubic interpolation is applied to enlarge one of the

downscaled images back to its original size, serving as input 1 for the auto-encoder network.

Simultaneously, spline interpolation is applied to another downscaled image. Spline interpolation aims to create a smooth and continuous estimate of pixel values in the enlarged image based on the existing pixel information. This technique involves constructing a smooth curve (spline) that passes through a set of given data points. Spline interpolation breaks the data into smaller intervals and fits separate low-degree polynomials in each interval, resulting in a piecewise continuous and smooth curve.

The interpolated image generated through spline interpolation serves as input 2 for the auto encoder network. Additionally, the downscaled image from the first step remains unchanged and is designated as input 3 for the auto-encoder network. Overall, these pre-processing steps, including downsampling, bicubic interpolation, and spline interpolation, aim to prepare the fingerprint images effectively for further processing within the auto-encoder network, facilitating feature extraction and super-resolution enhancement.

3.4. Proposed Deep Learning Classifier

The encoder and the decoder, as depicted in Figure 4, make up the two primary components of an auto encoder’s architecture. The auto encoder’s encoder component creates a lower-dimensional representation of the input data. It comprises several layers of neural network units, usually convolutional or dense layers, which progressively retrieve attributes from the input data. These layers reduce the input data’s dimensionality and capture its essential features. The encoder’s output is typically called latent space or bottleneck layer.

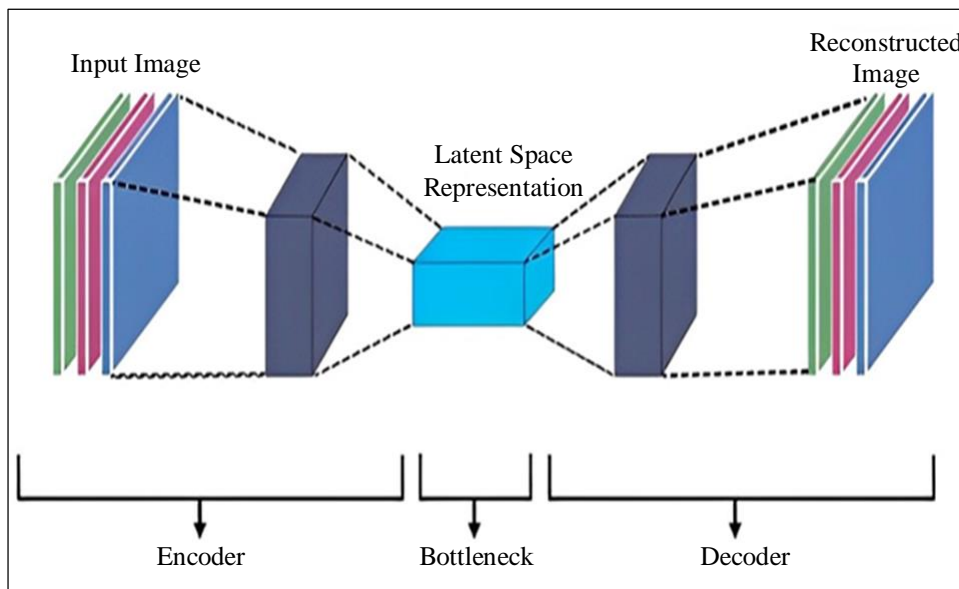


Fig. 4 General architecture of autoencoder

The decoder part reconstructs the original input data from the compressed representation generated by the encoder. Similar to the encoder, the decoder consists of multiple layers of neural network units arranged in a way that mirrors the encoder's structure but in reverse. These layers gradually expand the dimensions of the encoded representation back to the dimensions of the original input data. The decoder's output is the reconstructed version of the input data.

The auto encoder model utilized in the study incorporates three input layers, namely input1, input2, and input3. Each input layer undergoes feature extraction via two convolutional layers followed by maxpooling to reduce dimensionality. Specifically, input1 and input2 are processed through two convolutional layers separately, each applying 64 filters with a 3 x 3 kernel size and utilizing ReLu activation.

The subsequent maxpooling operation further reduces the dimensionality of the extracted features. Similarly, input3 undergoes feature extraction via two convolutional layers with the same specifications. Following feature extraction, the output images from the feature extraction steps for input1 and input2 are concatenated. Additionally, the output images from

all maxpooling operations are concatenated together. These concatenation steps ensure that both lower-level and higher-level features are effectively captured and preserved for further processing. The subsequent layer employs 128 filters with similar kernel size and activation functions. In the decoder part of the model, the concatenated output image from the maxpooling step is up-sampled. This up-sampled image is then concatenated with the output images from the previous concatenation step, combining both low-level and high-level features.

Finally, transposed convolution, also known as deconvolution, and is applied to generate the output image. This comprehensive auto-encoder architecture is designed to extract features effectively and reconstruct the input images, leveraging information from all three input layers to enhance the overall resolution and quality of the output image.

Additionally, the incorporation of two concatenation layers in the encoder ensures the preservation of fine image details during resolution enhancement, further contributing to the generation of high-quality output images. Table 2 displays the model summary for the proposed model.

Table 2. Model summary of the proposed model

Layer (Type)	Output Shape	Parameters
input_1 (Input Layer)	[(None, 258, 194, 3)]	0
input_2 (Input Layer)	[(None, 258, 194, 3)]	0
conv2d (Conv2D)	[(None, 258, 194, 64)]	1792
conv2d_2 (Conv2D)	[(None, 258, 194, 64)]	1792
input_3 (Input Layer)	[(None, 129, 97, 3)]	0
conv2d_1 (Conv2D)	[(None, 258, 194, 128)]	73856
conv2d_3 (Conv2D)	[(None, 258, 194, 128)]	73856
conv2d_4 (Conv2D)	[(None, 129, 97, 64)]	1792
max_pooling2d (Maxpoolind2D)	[(None, 129, 97, 128)]	0
max_pooling2d_1 (Maxpoolind2D)	[(None, 129, 97, 128)]	0
conv2d_5 (Conv2D)	[(None, 129, 97, 128)]	73856
concatenate_1 (Concatenate)	[(None, 129, 97, 384)]	0
concatenate (Concatenate)	[(None, 258, 194, 256)]	0
up_sampling2d (UpSampling2D)	[(None, 258, 194, 384)]	0
concatenate_2 (Concatenate)	[(None, 258, 194, 640)]	0
conv2d_transpose (Conv2DTranspose)	[(None, 258, 194, 3)]	17283
Total Parameters: 244227		
Trainable Parameters: 244227		
Non-Trainable Parameters: 0		

3.5. Finger Print Image Matching

A popular technique for matching images based on distinguishing important feature points is SIFT (Scale Invariant Feature Transform). It is particularly effective for fingerprint matching, where the images vary in scale, rotation, and illumination. SIFT works by detecting key points in the fingerprint images and describing their local neighbourhoods using gradient information. These feature points are typically local maxima in the image gradient magnitude and orientation, located at distinctive structures such as corners and edges. These key points exhibit resilience against alterations in dimensions and orientation, rendering them appropriate for image matching.

Once the key feature points are detected in both images, SIFT computes descriptors for each point based on the local image gradients. These descriptors encode information about the local image structure surrounding each key point. Matching is then performed by comparing the descriptors of corresponding key points between the original and reconstructed images. This comparison is usually done using Euclidean distance or other similarity metrics, with smaller distances indicating higher similarity.

On the other hand, FpMV (Fingerprint Minutiae Viewer) is an algorithm developed by the National Institute of Standards and Technology (NIST) specifically for fingerprint analysis [25]. FpMV focuses on detecting and measuring minutiae points in fingerprint images. Minutiae points are small, distinctive features such as ridge endings and bifurcations that are commonly used for fingerprint matching. FpMV identifies these minutiae points in both the original and reconstructed fingerprint images and analyses their spatial distribution and characteristics. By comparing the minutiae points between the two images, FpMV assesses the similarity and potential match between them.

SIFT and FpMV are two different algorithms used for fingerprint matching and analysis. While SIFT focuses on detecting and matching key feature points based on local image descriptors, FpMV specifically targets the detection and measurement of minutiae points in fingerprint images. Both methods play crucial roles in evaluating the accuracy and effectiveness of fingerprint reconstruction techniques by assessing the similarity and matching between reconstructed and original fingerprint images.

3.6. Performance Metrics

The performance of super-resolution algorithms is measured using both objective and subjective performance metrics parameters as follows [14].

3.6.1. Mean Squared Error (MSE)

MSE is a measure of the average squared difference between corresponding elements of an original image and a reconstructed image. The formula for Mean Squared Error is:

$$MSE = \sum_1^M \sum_1^N (X_{i,j} - Y_{i,j})^2 \quad (2)$$

Where M, N is the size of the image. $X_{i,j}, Y_{i,j}$ represents an actual and predicted value of pixels at i, j^{th} position.

3.6.2. Peak Signal to Noise Ratio (PSNR)

PSNR measures reconstruction fidelity by assessing MSE between the generated and ground truth images. PSNR inversely correlates with MSE, reflecting pixel-level differences rather than overall image quality. The PSNR is expressed in Decibels (dB) and is calculated using Equation 3.

$$PSNR = \frac{10 \log_{10}(2^n - 1)}{\sqrt{MSE}} \quad (3)$$

Where, 2^n is the maximum possible pixel value of the image, and MSE is the Mean Squared Error between the corresponding pixels of the original and reconstructed images. A higher PSNR value indicates a higher quality reconstruction, as it implies a lower level of distortion or noise.

3.6.3. Structural Similarity Index (SSIM)

The Structural Similarity Index is a metric used to measure the similarity between two images. SSIM considers structural information and attempts to mimic the human perception of image quality. The SSIM index ranges from -1 to 1, with 1 indicating perfect similarity. The SSIM is calculated by combining three components of the images. The formula for SSIM is given in Equation 4.

$$SSIM = \frac{(2 \mu_I \mu_K + C_1) * (2 \sigma_{IK} + C_2)}{(\mu_I^2 + \mu_K^2 + C_1) * (\sigma_I^2 + \sigma_K^2 + C_2)} \quad (4)$$

Where I and K are the two input images being compared, μ_I, μ_K are average luminescence values of I, K ; σ_I, σ_K are Variances of I and K ; σ_{IK} is Covariance of I and K ; and, C_1, C_2 are constants.

3.7. Hardware and Software Setup

The computational infrastructure is implemented on a robust machine equipped with an Intel Core i7 processor, 32GB of RAM, and an NVIDIA GeForce GTX 1080Ti GPU. Model development seamlessly unfolded through the Keras library [26], functioning as a prototype built upon the Tensorflow framework and executed using the versatile Python language. Leveraging Keras' user-friendly interface and potent capabilities, an intricate Neural Network architecture is designed. This framework ensures efficient resource utilization across CPU, GPU, and TPU environments. To harness extensive computational capabilities and streamline model training, the deployment is orchestrated on Google Colab, a cloud-based Python notebook environment offering complimentary access to robust computational resources and fostering collaborative development.

Hyperparameters are essential configuration settings that define the behavior and characteristics of a deep learning framework throughout the training process. Unlike the parameters of the model, which are learned from the data itself, hyperparameters are set by the user before training begins. The model configuration of the proposed approach is tabulated in Table 3.

Table 3. Hyper parameter specifications

Hyperparameters	Values
Epochs	30
Activation Function	ReLu, Sigmoid
Optimizer	ADAM
Loss Function	Binary Cross Entropy

4. Results and Discussion

Both objective and subjective performance metrics are utilized to assess the effectiveness of the suggested model against other state-of-the-art techniques. To evaluate the effectiveness of the proposed model in comparison to other state-of-the-art techniques, both objective and subjective performance indicators are used.

Subjective metrics rely on subjective judgment to assess image quality, whereas objective metrics are quantitative measurements that offer numerical assessments of the rebuilt images. The model’s performance is assessed using objective metrics, which are derived from the Human Visual System (HVS), as shown in Table 4.

Table 4. Performance metrics

Performance Metrics	Results Obtained
PSNR	0.968
SSIM	35.14
MSE	0.007

Comparing the suggested model to the actual images, these results imply that it achieves high structural similarity, PSNR, and low mean squared error. This suggests that the proposed approach effectively improves the quality of fingerprint images by producing reconstructions that closely resemble the originals with little distortion or information loss. Fingerprint identification using the SIFT algorithm is conducted on both the FVC 2004 and FVC 2002 datasets. The fingerprint images are analyzed using the SIFT technique to identify important feature points, which are then compared to identify individual fingerprints. As a result, all fingerprints in both datasets were properly matched with their respective IDs. The identification method yielded an accuracy of 100%.

Furthermore, Table 5 presents a comparison between the identification accuracy attained by the SIFT algorithm and the performance of various other cutting-edge techniques. The computational performance of the proposed model with respect to storage space is illustrated in Figure 5. The graph demonstrates that the proposed method excels in terms of model size when compared to existing state-of-the-art methods. This implies that the proposed model is more efficient in terms of storage space utilization, indicating potentially lower memory requirements and faster processing times.

Table 5. Accuracy comparison with the state-of-the-art methods using FVC 2004 Dataset

S. No.	Methodology	Year of Publishing	Accuracy (%)
1	Gabor Filter	2020 [27]	94.09
2	Convolution Neural Network	2020 [12]	80
3	Convolution Autoencoder Network	2021 [5]	95.02
4	Convolutional Deep Autoencoder	2022 [28]	94.1
5	Convolution Neural Network Combined with Edge Filters	2022 [29]	75.6
6	Proposed Methodology		100

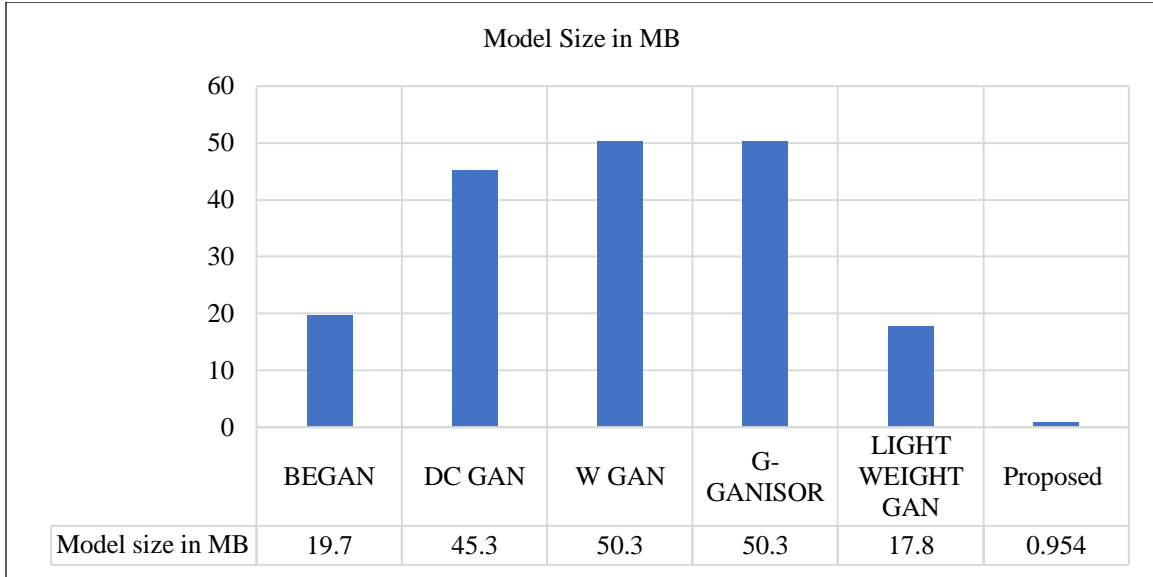


Fig. 5 Model size comparison with the existing methods

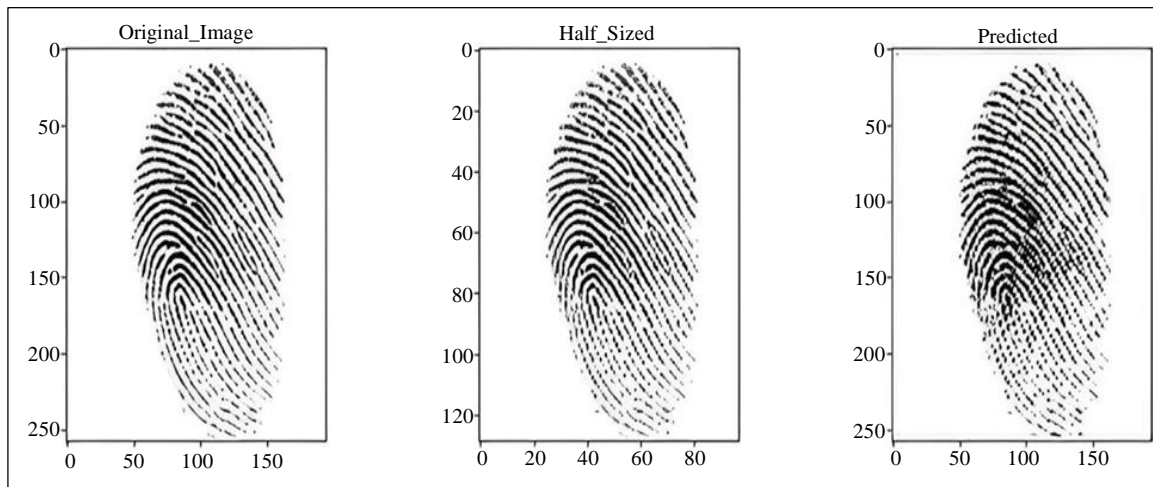
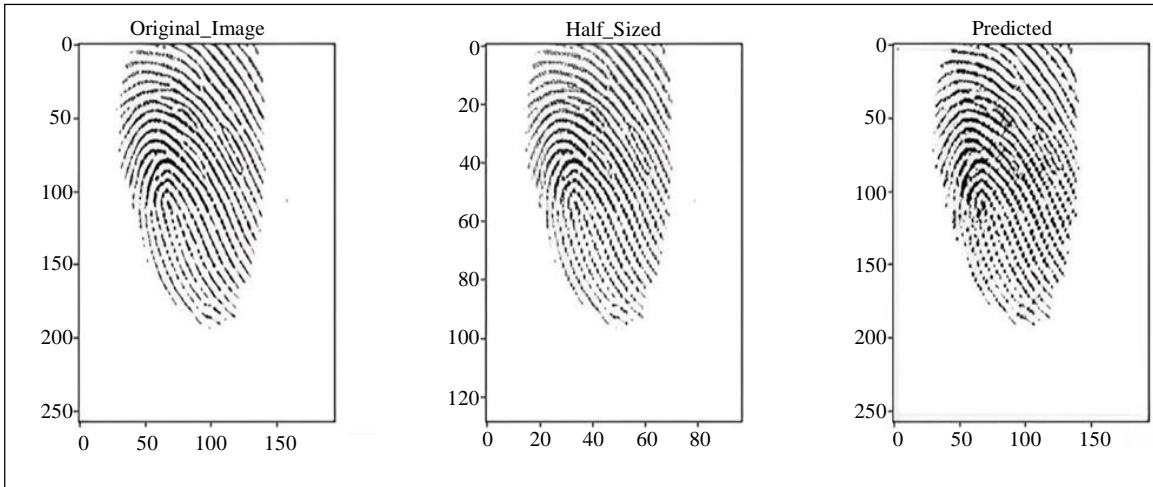


Fig. 6 Ground-truth image, half-sized image and regenerated image using FVC 2004

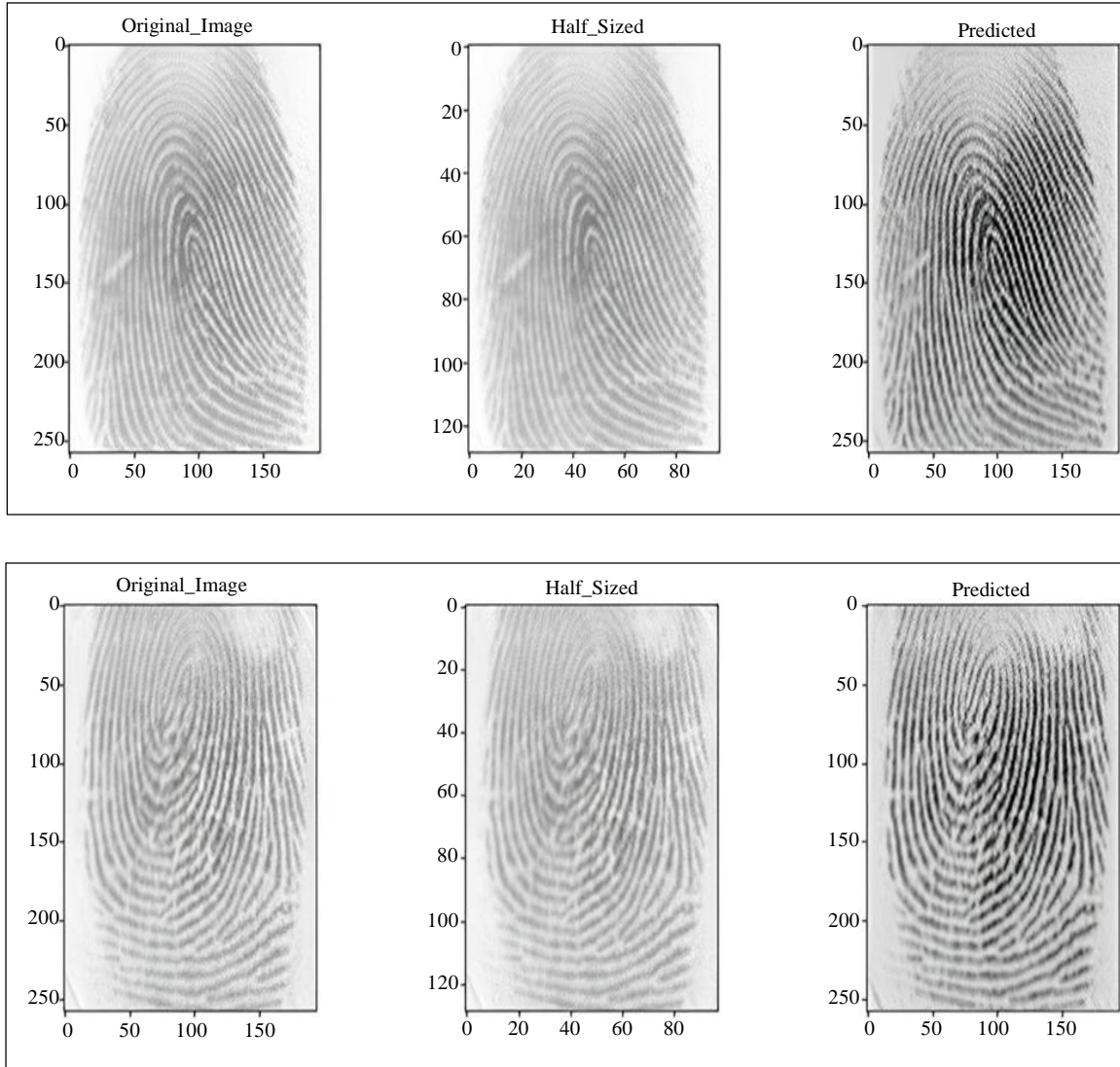


Fig. 7 Ground-truth image, half-sized image and regenerated image using FVC 2002

Figures 6 and 7 depict the input and output images, respectively, for randomly selected samples from a standard dataset. These images serve as illustrative examples to showcase the efficiency of the proposed model in enhancing the quality of fingerprint images.

Figure 8 illustrates the key points identified in both the original image and the generated image. These key points are crucial landmarks or features extracted from the fingerprint patterns, which play a significant role in fingerprint recognition and matching algorithms.

A close correspondence between the key points in the original and generated images indicates that the proposed model successfully retains essential fingerprint characteristics, leading to improved image quality and enhanced recognition accuracy.

Figure 9 illustrates the matching procedure between the ground-truth fingerprint image and the generated image using the SIFT algorithm. This process involves identifying and aligning corresponding key feature points between the two images to assess their similarity and evaluate the accuracy of the generated image.

In Figure 9, the matching procedure is visualized through lines connecting corresponding feature points between the ground truth and generated images. Each line represents a successful match between a pair of feature points, indicating their similarity and alignment.

The quality of the matching is assessed based on factors such as the number of successful matches, the accuracy of the alignment, and the overall consistency between the two images.

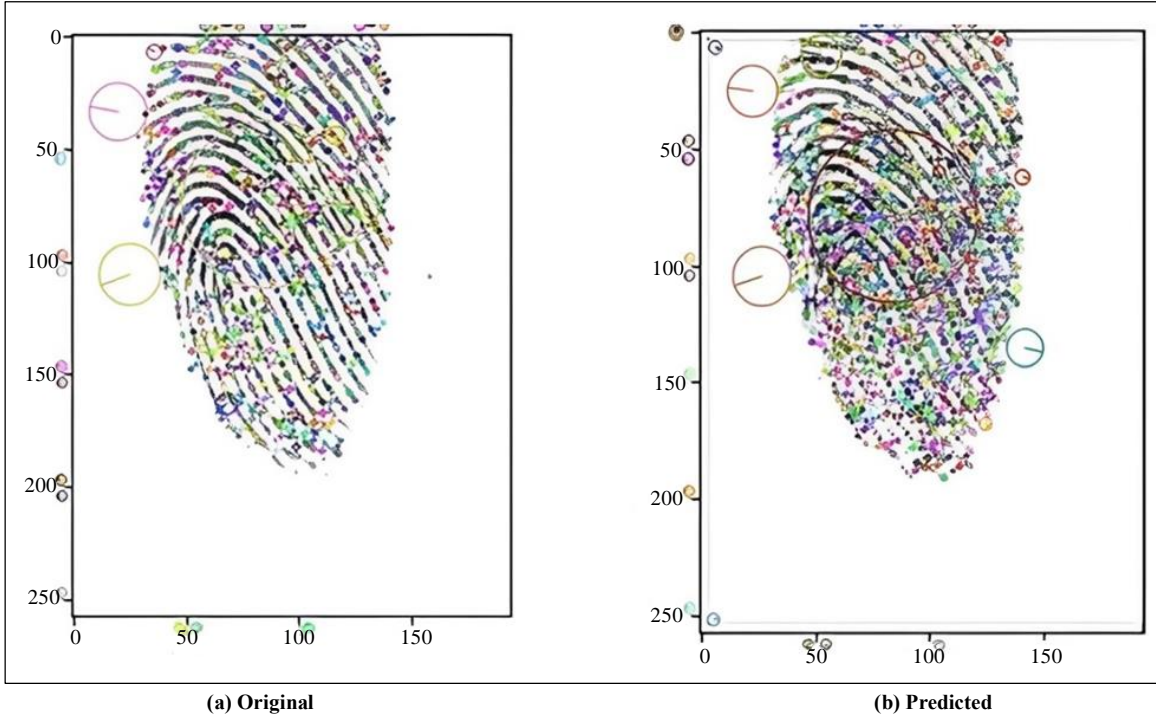


Fig. 8 Key feature points detected in original and regenerated image using the FpMV method

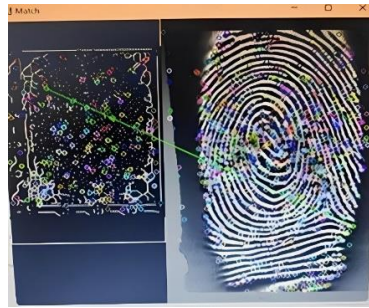


Fig. 9 Image matching using SIFT method

5. Conclusion

The increasing demand for enhanced image quality and finer details has underscored the importance of super-resolution techniques across various sectors, including scientific, medical, industrial, and entertainment domains. This study focuses on enhancing the resolution of fingerprint images by doubling their original size using an auto-encoder network combined with spline and bi-cubic interpolation techniques. The process involves the parallel application of spline and bi-cubic interpolation on down-sampled input images to extract all relevant features while preserving prominent characteristics.

By incorporating the concatenation of channels in both the encoder and decoder, the model successfully regenerates high-quality output images while maintaining important features. Evaluation using the SIFT algorithm demonstrates a 100% identification accuracy when comparing the enhanced images with ground-truth counterparts. Additionally, the

number of minutiae points extracted from the regenerated images, measured using the FpMV algorithm, and surpasses those from the ground truth, indicating superior image quality.

Furthermore, performance metrics such as PSNR, SSIM, and MSE values validate the efficacy of the proposed method compared to existing techniques. As a potential future direction, this model could be extended to enhance fingerprints obtained from crime scenes, contributing to advancements in forensic investigations.

Acknowledgements

I would like to express my sincere gratitude to all those who contributed to the completion of this research paper. I extend my heartfelt thanks to my supervisor, Jayasree V K, for their invaluable guidance and unwavering support throughout the research process. I extend my thanks to my family, my colleagues and fellow researchers for their encouragement and understanding during the demanding phases of this work.

References

- [1] Davide Maltoni et al., *Handbook of Fingerprint Recognition*, 2nd ed., Springer London, 2009. [[CrossRef](#)] [[Google Scholar](#)] [[Publisher Link](#)]
- [2] Weixin Bian, Shifei Ding, and Yu Xue, "Fingerprint Image Super Resolution Using Sparse Representation with Ridge Pattern Prior by Classification Coupled Dictionaries," *IET Biometrics*, vol. 6, no. 5, pp. 342-350, 2017. [[CrossRef](#)] [[Google Scholar](#)] [[Publisher Link](#)]
- [3] Patrick Schuch, Simon Schulz, and Christoph Busch, "Survey on the Impact of Fingerprint Image Enhancement," *IET Biometrics*, vol. 7, no. 2, pp. 102-115, 2018. [[CrossRef](#)] [[Google Scholar](#)] [[Publisher Link](#)]
- [4] Kshitij Singh, and Gireesh Kumar Dixit, "Application of Machine Learning in Fingerprint Image Enhancement and Recognition: A Review," *Smart Moves Journal Ijoscience*, vol. 7, no. 4, pp. 33-37, 2021. [[Google Scholar](#)] [[Publisher Link](#)]
- [5] Sergio Saponara, Abdussalam Elhanashi, and Qinghe Zheng, "Recreating Fingerprint Images by Convolutional Neural Network Autoencoder Architecture," *IEEE Access*, vol. 9, pp. 147888-147899, 2021. [[CrossRef](#)] [[Google Scholar](#)] [[Publisher Link](#)]
- [6] Anand Deshpande, and Prashant P. Patavardhan, "Survey of Super Resolution Techniques," *ICTACT Journal on Image & Video Processing*, vol. 9, no. 3, pp. 1927-1934, 2019. [[CrossRef](#)] [[Google Scholar](#)] [[Publisher Link](#)]
- [7] Sen Wang, and Yangsheng Wang, "Fingerprint Enhancement in the Singular Point Area," *IEEE Signal Processing Letters*, vol. 11, no. 1, pp. 16-19, 2004. [[CrossRef](#)] [[Google Scholar](#)] [[Publisher Link](#)]
- [8] Alexandre Boucher, Phaedon C. Kyriakidis, and Collin Cronkite-Ratcliff, "Geostatistical Solutions for Super-Resolution Land Cover Mapping," *IEEE Transactions on Geoscience and Remote Sensing*, vol. 46, no. 1, pp. 272-283, 2008. [[CrossRef](#)] [[Google Scholar](#)] [[Publisher Link](#)]
- [9] Kamal Nasrollahi, and Thomas B. Moeslund, "Super-Resolution: A Comprehensive Survey," *Machine Vision and Applications*, vol. 25, pp. 1423-1468, 2014. [[CrossRef](#)] [[Google Scholar](#)] [[Publisher Link](#)]
- [10] Yoong Khang Ooi, and Haidi Ibrahim, "Deep Learning Algorithms for Single Image Super-Resolution: A Systematic Review," *Electronics*, vol. 10, no. 7, pp. 1-33, 2021. [[CrossRef](#)] [[Google Scholar](#)] [[Publisher Link](#)]
- [11] Wenming Yang et al., "Deep Learning for Single Image Super-Resolution: A Brief Review," *IEEE Transactions on Multimedia*, vol. 21, no. 12, pp. 3106-3121, 2019. [[CrossRef](#)] [[Google Scholar](#)] [[Publisher Link](#)]
- [12] Uttam U. Deshpande et al., "End-to-End Automated Latent Fingerprint Identification with Improved DCNN-FFT Enhancement," *Frontiers in Robotics and AI*, vol. 7, pp. 1-18, 2020. [[CrossRef](#)] [[Google Scholar](#)] [[Publisher Link](#)]
- [13] Jeremy Vonderfecht, and Feng Liu, "Fingerprints of Super Resolution Networks," *Transactions on Machine Learning Research*, pp. 1-14, 2022. [[Google Scholar](#)] [[Publisher Link](#)]
- [14] Juan E. Tapia et al., "Selfie Periocular Verification Using an Efficient Super-Resolution Approach," *IEEE Access*, vol. 10, pp. 67573-67589, 2022. [[CrossRef](#)] [[Google Scholar](#)] [[Publisher Link](#)]
- [15] Young Won Lee, Jung Soo Kim, and Kang Ryoung Park, "Ocular Biometrics with Low-Resolution Images Based on Ocular Super-Resolution CycleGAN," *Mathematics*, vol. 10, no. 20, pp. 1-30, 2022. [[CrossRef](#)] [[Google Scholar](#)] [[Publisher Link](#)]
- [16] M.B. Shahbakhsh, and H. Hassanpour, "Empowering Face Recognition Methods Using a GAN-Based Single Image Super-Resolution Network," *International Journal of Engineering*, vol. 35, no. 10, pp. 1858-1866, 2022. [[CrossRef](#)] [[Google Scholar](#)] [[Publisher Link](#)]
- [17] Wazir Muhammad et al., "Multi-Path Deep CNN with Residual Inception Network for Single Image Super-Resolution," *Electronics*, vol. 10, no. 16, pp. 1-25, 2021. [[CrossRef](#)] [[Google Scholar](#)] [[Publisher Link](#)]
- [18] Chi-En Huang et al., "Super-Resolution Generative Adversarial Network Based on the Dual Dimension Attention Mechanism for Biometric Image Super-Resolution," *Sensors*, vol. 21, no. 23, pp. 1-22, 2021. [[CrossRef](#)] [[Google Scholar](#)] [[Publisher Link](#)]
- [19] Vijay Anand, and Vivek Kanhangad, "PoreNet: CNN-Based Pore Descriptor for High-Resolution Fingerprint Recognition," *IEEE Sensors Journal*, vol. 20, no. 16, pp. 9305-9313, 2020. [[CrossRef](#)] [[Google Scholar](#)] [[Publisher Link](#)]
- [20] Ngoc Tuyen Le et al., "Fingerprint Enhancement Based on Tensor of Wavelet Subbands for Classification," *IEEE Access*, vol. 8, pp. 6602-6615, 2020. [[CrossRef](#)] [[Google Scholar](#)] [[Publisher Link](#)]
- [21] Dogus Karabulut et al., "Cycle-Consistent Generative Adversarial Neural Networks Based Low Quality Fingerprint Enhancement," *Multimedia Tools and Applications*, vol. 79, pp. 18569-18589, 2020. [[CrossRef](#)] [[Google Scholar](#)] [[Publisher Link](#)]
- [22] FVC2002, Fingerprint Verification Competition, Databases, 2002. [Online]. Available: <http://bias.csr.unibo.it/fvc2002/databases.asp>
- [23] FVC2004, Fingerprint Verification Competition, Databases, [Online]. Available: <http://bias.csr.unibo.it/fvc2004/databases.asp>
- [24] K.T. Gribbon, and D.G. Bailey, "A Novel Approach to Real-Time Bilinear Interpolation," *Proceedings. DELTA 2004. Second IEEE International Workshop on Electronic Design, Test and Applications*, Perth, Australia, pp. 126-131, 2004. [[CrossRef](#)] [[Google Scholar](#)] [[Publisher Link](#)]
- [25] <https://www.nist.gov/services-resources/software/org/>
- [26] Antonio Gulli, Amita Kapoor, and Sujit Pal, *Deep Learning with TensorFlow 2 and Keras: Regression, ConvNets, GANs, RNNs, NLP, and more with TensorFlow 2 and the Keras API*, 2nd ed., Packt Publishing, Birmingham, 2019. [[Google Scholar](#)] [[Publisher Link](#)]
- [27] A.T. Gowthami, and H.R. Mamatha, "Fingerprint Recognition Using Zone Based Linear Binary Patterns," *Procedia Computer Science*, vol. 58, pp. 552-557, 2015. [[CrossRef](#)] [[Google Scholar](#)] [[Publisher Link](#)]

- [28] Andreea-Monica Dincă Lăzărescu, Simona Moldovanu, and Luminita Moraru, "A Fingerprint Matching Algorithm Using the Combination of Edge Features and Convolution Neural Networks," *Inventions*, vol. 7, no. 2, pp. 1-13, 2022. [[CrossRef](#)] [[Google Scholar](#)] [[Publisher Link](#)]
- [29] Rashmi Gupta et al., "Fingerprint Image Enhancement and Reconstruction Using the Orientation and Phase Reconstruction," *Information Sciences*, vol. 530, pp. 201-218. 2020. [[CrossRef](#)] [[Google Scholar](#)] [[Publisher Link](#)]